

Collision Cross Sections of Carbon and Hydrogen for Fast Neutrons

WILLIAM SLEATOR, JR.*

Department of Physics, University of Michigan, Ann Arbor, Michigan

(Received March 17, 1947)

Experiments are described by means of which the collision cross sections of carbon and hydrogen were determined for neutrons of nine different energies between 6 Mev and 22 Mev. The experimental method was such that data could be taken on groups of neutrons having energies within an interval small compared to the neutron energy, and at any energy produced by an energy heterogeneous source. The results are consistent with those of other observers at the four neutron energies in this range which have been previously investigated. A comparison with various theories shows that at high energies the observed hydrogen cross sections are about 10 percent larger than pure *S*-wave cross sections computed on the basis of a square well interaction between neutron and proton, and that they agree very well with the "symmetrical" theory of Rarita and Schwinger.

1. INTRODUCTION

NEUTRON sources in the 5- to 25-Mev energy range available up to 1943, when the present experiments were carried out, produced neutrons distributed continuously in energy. Therefore, in order to measure cross sections for neutrons in energy intervals small compared to the neutron energy, it was necessary to use a detecting system which could discriminate against neutrons outside of a particular interval. The first method which accomplished this made use of a nuclear reaction with a definite energy threshold as neutron detector. In this case, the most energetic neutrons produced by the source must be a reasonable interval above the detector threshold, and the method is limited to those energies at which there are suitable threshold reactions. It has been used at 7 Mev by Grahame and Seaborg¹ with $\text{Fe}^{56}(n, p)\text{Mn}^{56}$, at 12 Mev by Salant and Ramsey² with $\text{Cu}^{63}(n, 2n)\text{Cu}^{62}$, and at 21 Mev by Sherr³ with $\text{C}^{12}(n, 2n)\text{C}^{11}$.

Aside from the present results, the only other total cross-section data known to the writer on neutrons above 6 Mev are those of Ageno, Amaldi, Bocciarelli, and Trabacchi.⁴ They measured the cross sections of hydrogen, deuterium,

and carbon at 4.1, 12.5, and 13.5 Mev with neutrons from Be, B, and Li targets, respectively, bombarded with 1-Mev deuterons. Their detecting method was similar in principle to that of the present experiments. However, since only 1-Mev deuterons were available, they were restricted to energies near those released in the nuclear reactions.

A very complete study of the cross sections of carbon, hydrogen, deuterium, and oxygen between 0.35 Mev and 6.0 Mev has been made by Bailey *et al.*⁵ Above 2 Mev, these workers also used a heterogeneous neutron source and a differential method, somewhat different from that described below, to observe the effects of the neutrons in small energy intervals.

The results obtained by these observers on carbon and hydrogen for neutron energies greater than 5 Mev are shown in Figs. 3 and 4, along with the results of the present experiments. Theoretical work relating data of this sort to the problem of nuclear forces will be referred to, and the experimental results compared with those of various theories, in the last section of the paper.

2. EXPERIMENTAL METHOD AND APPARATUS

The fast neutron collision cross section of a nucleus can be determined most easily by means of a transmission experiment, that is, one in which the fraction of a neutron beam is measured

* Now at the University of Minnesota.

¹ D. C. Grahame and G. T. Seaborg, *Phys. Rev.* **53**, 795 (1938).

² E. O. Salant and N. F. Ramsey, *Phys. Rev.* **57**, 1075A (1940).

³ R. Sherr, *Phys. Rev.* **68**, 240 (1945).

⁴ M. Ageno, E. Amaldi, D. Bocciarelli, and G. C. Trabacchi, *Naturwiss.* **31**, 231 (1943); *Phys. Rev.* **71**, 20 (1947).

⁵ Carl L. Bailey, W. E. Bennett, Thor Bergstrahl, R. G. Nuckolls, H. T. Richards, and J. H. Williams, *Phys. Rev.* **70**, 583 (1946); **70**, 805 (1946).

which a known amount of the element transmits unaltered in direction and in energy. In general, cross sections obtained in this way will be the sum of cross sections for three different processes: elastic scattering, inelastic scattering, and radiative capture. However, the capture cross sections of both hydrogen and carbon for neutrons of the energies dealt with in the present experiment are negligible.⁶ In the case of hydrogen, moreover, inelastic scattering does not take place, so that a transmission measurement will give just the total scattering cross section appropriate for comparison with theory. The result of this kind of experiment will not make possible the separate evaluation of the two cross sections for carbon unless some other information can also be used. (This question is discussed below in Section 4.) Transmission measurements are particularly advantageous when the source is such that the detector must define the energy interval, since in a transmission experiment the detector need not be altered in any way between the beam strength measurements to be compared, and its energy response will necessarily be the same. Thus the method is free of the source of error which has been most serious for angular distribution measurements.**

Neutrons for the present experiments were obtained by bombarding beryllium and lithium with 10-Mev deuterons produced by the Michigan cyclotron. In the first case the reaction is $\text{Be}^9 + \text{D}^2 \rightarrow \text{B}^{10} + n^1$, and the most energetic neutrons had about 14-Mev energy. Neutrons from this reaction were used to study three energy intervals between 6 and 11 Mev. They were not used at higher energies because of the relatively small number near the upper energy limit. The

lithium reaction, $\text{Li}^7 + \text{D}^2 \rightarrow \text{Be}^4 + n^1$, produced neutrons having energies up to about 25 Mev, with which 7 energy intervals between 10 and 23 Mev were investigated.

The detecting method used was one which will determine the number of neutrons in an energy interval of almost arbitrary size at any energy. The essence of the method is this: the protons in any energy interval, which are knocked out of a thin paraffin layer at a particular angle, are all due to neutrons in a corresponding but slightly larger energy interval. (The neutron energy interval is larger by a small factor depending on the scattering angle and also by an additive amount equal to the energy which a proton can lose in going through the paraffin layer.) The intensity of the neutron beam is measured, in units of unknown but constant absolute magnitude, by counting these recoil protons. To determine the neutron intensity in a particular energy interval it is necessary to take the difference between two sets of counts during which the same number of neutrons, distributed in the same way with respect to energy, are produced by the source. This can be approximated by keeping conditions at the source constant, and then measuring while two equal charges of deuterons fall on the cyclotron target. Between the paraffin layer and the ionization chamber are placed aluminum absorbers such that one of these sets of counts measures the total number of neutrons having energies above the lower limit of the interval, while the other measures the number which have energies above the upper limit of the interval.

The efficiency of this system is necessarily low because only a very small fraction of the neutrons will collide with protons in a layer of paraffin thin enough so that there will be a relatively small energy difference between protons produced on the two sides of the layer by neutrons of the same energy. Also, unless the angles subtended by the detector at the paraffin layer and by the paraffin layer at the detector are small, a large energy spread will be introduced by the collisions which occur at widely different angles. Thus the number of protons observed is small, and it is important to have as large a ratio as possible between the pairs of counts whose difference is to be taken. When the Li target was

⁶ H. A. Bethe, *Rev. Mod. Phys.* **9**, 160 (1937).

** For example, in the latter experiments on hydrogen (references 7 and 8), the recoil proton intensity is measured at two different angles with respect to the neutron beam, and the angular distribution is then inferred from a comparison of these two intensities. If the comparison is to be significant, the neutron energy intervals used at the two angles must be exactly the same because the neutron intensity in the interval depends very strongly on where the interval is cut off at the low energy end. This means that the proton cut-off energy will have to be different at the two angles by exactly the right amount. This adjustment can cause serious errors because, for example, it depends quantitatively on the somewhat uncertain range-energy relation of protons in aluminum.

⁷ Howard Tatel, *Phys. Rev.* **61**, 450 (1942).

⁸ E. Amaldi, D. Bocciarelli, B. Ferretti, and G. C. Trabacchi, *Naturwiss.* **30**, 582 (1942).

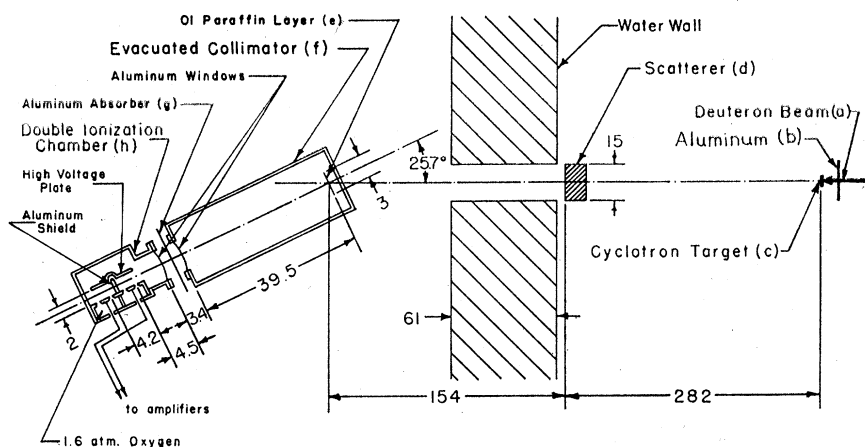


FIG. 1. Arrangement of apparatus, Be target in cyclotron. When the Li target was used, the angle between neutron and proton paths was 31.4° , the paraffin layer was 0.028 cm thick and 32.7 cm from the ionization chamber, and the collimator was not used.

NOTE: DIMENSIONS IN CM
NOT TO SCALE.

used, the largest values of this ratio occurred when the upper limit of the interval was somewhere near the energy of the most energetic neutrons produced by the source. In general, therefore, enough Al was put in front of the Li target in the cyclotron to bring about an approximate coincidence of these two energies. Under these conditions, a thick paraffin layer would do as well as a thin one, since only those protons losing very little energy in the paraffin would be able to get through the Al absorbers.

However, with neutrons from the Be target the best values of this ratio occurred when the upper limit of the energy interval was several Mev below the peak energy of the source. Also, in order to work on the 9–13-Mev region with the more abundant Li neutrons, it was necessary to cut off the energy interval below the peak energy of the source, which could not be made as low as the 14 Mev released in the reaction. Therefore a thin paraffin layer (one in which the protons lost on the average about $\frac{1}{2}$ Mev) was used, making it possible for the detector to put an upper as well as a lower limit on the working energy interval.

The arrangement of the apparatus is shown schematically in Fig. 1 for the low energy runs in which beryllium was used as the cyclotron target. The set-up used at high energies with the lithium target differed from this only in the respects noted below. The following lettered remarks correspond to the letters in the figure.

(a) The arrow represents the deuteron beam

produced by the cyclotron, with energy about 10 Mev and intensity 8–15 microamperes.

(b) This line represents the aluminum absorbers of various thicknesses which were put in front of the target during most of the runs with Li to slow down the deuterons.

(c) The cyclotron target was a piece of beryllium or lithium about 3.0 cm. wide, 2.0 cm high, and 0.4 cm thick, screwed tightly to the water-cooled brass target cup. The dimensions of the effective neutron source, i.e., the part of the target receiving most of the deuteron beam, were about 2.0 cm horizontally and 0.4 cm vertically.

(d) The scatterers were blocks of graphite or paraffin about 15 cm square, set up 282 cm from the cyclotron target and 154 cm from the paraffin layer. Various thicknesses were used. The determination of their composition and density will be described in the next section.

(e) The paraffin layer from which protons were knocked by a small fraction of the neutrons was, for the runs with the Be target 9 cm high, 3 cm wide (perpendicular to the recoil protons), and 0.01 cm thick. When Li was used as the cyclotron target, the layer was 12 cm high, 2 cm wide, and 0.028 cm thick.

(f) At low energies an evacuated box, labeled "collimator," with an aluminum window to let the protons out, contained the paraffin layer and extended nearly to the ionization chamber. Its angle and length were such as to put the ionization chamber outside of the direct neutron beam (in order to cut down the number of recoiling

nuclei in the chamber), and to cause the sensitive region of the chambers to subtend a sufficiently small angle at the paraffin layer so as not to widen the energy interval intolerably. At the higher energies this box was omitted, and an air space of 32.7 cm took the place of some of the aluminum absorber. In this case the center of the proton beam made an angle of 31.4° with that of the neutron beam. The minimum proton energy necessary to cause a coincidence is computed for the two cases in Table I of Section 3.

(g) The aluminum absorbers defining the limits of the energy intervals were put into the proton path at this line. The thicknesses used, and the resulting proton and neutron energies, are shown in Table II of Section 3.

(h) The double ionization chamber and circuits arranged to record only coincidences were necessary because in a single chamber the background count in the cyclotron room was much too high. The chamber and circuits will now be described.

The coincidence ionization chamber was built and used by H. Tatel to measure the angular distribution of protons scattered by 11-Mev neutrons. Its construction has been described in Tatel's article,⁷ so that for our purposes a statement of the critical dimensions and the conditions under which it was used in the present experiments will be sufficient. The general shape and most of the dimensions can be seen in Fig. 3.

Each of the two sensitive regions is 4 cm high, 2 cm wide in the direction of the electric field, and 2.3 cm deep along the proton path. Corresponding points in the two chambers are 4.2 cm apart along the proton path. Between them, perpendicular to the proton path, is a thin aluminum shield. The protons entered the chamber through an aluminum window (1 mil thick for the low energy runs and 2 mils thick for those at high energy), and then had to travel 4.5 cm before reaching the sensitive region of the first chamber. Throughout the present experiments the chambers were filled with oxygen at 1.6-atmospheres pressure, and the ion collecting potential was about 5700 volts. A test of the dependence of the counting rate on the collecting voltage showed that with the electrical sensitivity at its standard value, and an oxygen pressure of 1.6 atmos., the voltage had to drop

below 5100 before the counting rate decreased observably.

The low voltage collecting plate of each chamber was connected to the first grid of a four stage resistance-capacitance coupled pulse amplifier, the gain of which could be varied. The amplifiers were connected through discriminators to a Rossi coincidence circuit, the output of which went to a scaling circuit and mechanical counter. The coincidence resolving time of this system was measured by Tatel with alpha-particle sources of various strengths and found to be 1.2×10^{-4} seconds.

Since the method used to determine transmission fractions required that all protons which passed through the chambers be counted, it was necessary to measure the over-all sensitivity of the counting systems to discover what proton energies were allowable. Accurately reproducible settings of the electrical sensitivity, which depended on the relation between amplifier gain and discriminator bias, were made by means of an 1000-cycle oscillator in the manner described by Tatel. The operating value was taken to be the most sensitive setting at which no noise pulses were counted (this test was made with the cyclotron running). Then the over-all sensitivity of each counting system, i.e., the minimum energy loss a particle must have in the sensitive region of the chamber in order to produce a countable pulse, was determined by tests made at reduced pressure with polonium alpha-particles. The first chamber and its circuits were found to be such that under operating conditions (electrical sensitivity as above, 1.6 atmos. O_2 , and 5700 volts) a particle would be counted if it lost more than 78 kev/cm in the sensitive region. This is equivalent to 44 kev/cm in standard air, so that the most energetic protons which the first chamber could count were those which had about 11.6 Mev as they entered the sensitive region. (For alpha-particles the range-energy relation given by Holloway and Livingston⁹ was used, and for protons that of Livingston and Bethe.¹⁰) To be detected by the second chamber and its circuits, a particle had to lose 73 kev/cm

⁹ M. G. Holloway and M. S. Livingston, *Phys. Rev.* **54**, 31 (1938).

¹⁰ M. S. Livingston and H. A. Bethe, *Rev. Mod. Phys.* **9**, 268 (1937).

or 168 kev in the 2.3 cm long sensitive region. This is the energy loss of a proton in the last 0.24 air cm of its range, so that the least energetic protons which could cause coincidences were those whose paths ended about 0.24 air cm inside the sensitive region of the second chamber. These protons had about 2.5 Mev as they entered the sensitive region of the first chamber.

Thus the system as it was used would count any protons which, as they entered the sensitive region of chamber 1, had energies between 2.5 Mev and 11.6 Mev. Because of the curvature of the range-energy relation, this will correspond to a smaller energy difference in the protons before they have passed through the Al absorbers. However, the initial energy range of the protons which the chambers could count was ample even for those cases in which a working interval was used, the upper limit of which was several Mev below the energy of the fastest neutrons produced by the source.

3. MEASUREMENTS

The composition of the paraffin scatterers was determined by means of melting point measurements. Two samples of the paraffin changed from completely liquid to completely solid between 60° and 56°C. This implies an average chain length of 26.6 carbons, and gives for the ratio, f , of the number of H atoms to the number of C atoms, $f = 2.075 \pm 0.2$ percent. The scatterers used were two blocks of this paraffin about 6 inches square and $1\frac{1}{2}$ inches thick. The surfaces through which the neutrons were to pass were scraped flat and parallel (to ± 0.001 inch) with a steel straight edge. Measurements of size and mass gave the mass per unit area to within 0.1 percent. For one block this was 3.163 g/cm², and for the other, 3.139 g/cm². The graphite used for the carbon scatterers was obtained from the National Carbon Company of Cleveland, and according to their analysis contained less than 0.1 percent of substances other than carbon. It was in the form of pieces $\frac{1}{2}$ inch thick and 6 inches square whose surfaces had been machined flat and parallel, and the mass per unit area of each was determined as above.

The calculation and final values of the neutron energy intervals used are shown in Tables I and

II. These may be made clearer by the following remarks.

The difference between two counts will give the number of recoil protons in an energy interval ($E_{p0} - E_{p1}$) which has been sharply cut off at both ends by the aluminum absorbers. The lower and upper limits, E_0 and E_4 , of the neutron energy interval to which this corresponds are given by the expressions

$$E_0 = E_{p0}/\cos^2\theta_0, \quad E_4 = (E_{p1} + \Delta E_p)/\cos^2\theta_2.$$

Here θ_0 is the minimum angle, and θ_2 the maximum angle, between the paths of neutron and proton at which the proton can reach the ionization chamber, and ΔE_p is the energy a proton loses in going all the way through the paraffin layer. The probability that a neutron of a particular energy will produce a proton in the interval $E_{p0} - E_{p1}$, i.e., the efficiency of the neutron detector, is not the same for all neutron energies between E_0 and E_4 , but behaves somewhat like the solid curve in Fig. 2. The dotted curve shows how it would look if $\theta_2 = \theta_0$ and $\Delta E_p = 0$. Here $E_1 = E_{p1}/\cos^2\theta_0$.

The actual effective energy distribution of the neutrons in an interval is the product of this detector efficiency and the distribution function of the neutrons produced by the source. Since this function was always greater at the low energy end of the interval, the effective neutron energy is lower than the center of the efficiency curve. The available information about the neutron distribution was sufficient to justify a guess at the effective neutron energy for each interval (last column of Table II) but not to locate it exactly.

At each new energy interval, various Al thicknesses were tried in the target cup, and sometimes the absorbers in front of the chamber were also changed, until what appeared to be the optimum combination was discovered. The criterion used in making this adjustment was not the relative position of the upper limit of the interval and the peak energy of the source (though in the runs on lithium these probably coincided fairly closely) but the ratio of the number of neutrons (per deuteron) in the interval to the number above it.

When this adjustment was such as to produce an adequate ratio for an appropriate energy

interval, the fraction of the neutrons transmitted in this interval by a particular scatterer could be determined. In the discussion of this process the word "count" will mean a determination of the number of coincidences which occur while a definite number of deuterons, measured in arbitrary but constant integrator units, fall on the cyclotron target, for a particular configuration of scatterer and absorbers (e.g., scatterer in the beam and upper limit absorber in front of chamber). A "run" is a determination of the transmission fraction of a particular scatterer for the neutrons in a particular interval, and always consists of several of each of four different kinds of counts. The scatterer-absorber arrangements for these counts are (a) lower limit absorber in front of chamber and scatterer not in beam, (b) upper limit absorber in front of chamber and scatterer not in beam, (c) and (d), similar to (a) and (b), respectively, but with the scatterer in the beam. Let A be the total number of coincidences observed, and N_A the total number of integrator units of deuterons striking the cyclotron target during all the counts of type (a) in a run, and let B , N_B , C , N_C , D , and N_D be the corresponding quantities for counts of the other three types. Then the observed fraction T_{obs} of the neutrons in the working interval transmitted by the scatterer is given by

$$T_{\text{obs}} = \frac{C/N_C - D/N_D}{A/N_A - B/N_B}.$$

It would have been desirable, of course, to measure the length of a count in terms of the number of neutrons in the working energy

interval produced by the source, but this would have required essentially another complete detecting system. Instead, the length of a count was measured in terms of the charge of deuterons falling on the cyclotron target by means of a current integrator attached to the latter. The number of "integrator units" of deuterons was proportional to the number of neutrons produced as long as cyclotron operating conditions were kept absolutely constant. The two factors which were observed to have the greatest effect on this ratio were (1) the strength of the magnetic field, which affected the energy of the deuterons, and (2) the pressure in the cyclotron tank on which the energy distribution of the deuterons depended. Numerous tests showed that by careful adjustment and operation of the cyclotron these things could be kept effectively constant during times the order of 30 minutes, but seldom for as much as an hour. Therefore, it was desirable to take at least one of each of the 4 kinds of counts about every half hour. Since the number of coincidences occurring in a count of 5 to 10 minutes was in general not nearly large enough to produce a sufficiently accurate value of the transmission fraction, at least 5, and usually 8 or 10, counts of each kind were taken during each run. The value of T_{obs} from each run is given in Tables III and IV, Section 4. The relative standard deviation in T_{obs} , ΔT , given in these tables was computed on the assumptions that the standard deviation in each of the numbers A and B was equal to its square root, that the uncertainty in N_A and N_B was negligible, and that $N_B = N_A$ and $N_D = N_C$. (This latter condition was nearly always and always nearly fulfilled.) The ex-

TABLE I. Range of countable protons of least energy.

	Be target (as in Fig. 1)	Li target
Aluminum window, collimator:	0.001 inch or 7.35 mgm/cm ²	0 mgm/cm ²
Aluminum window, detector:	0.001 inch or 7.35 mgm/cm ²	13.6 mgm/cm ²
Aluminum internal shield detector:	0.0007 inch or 4.30 mgm/cm ²	4.3 mgm/cm ²
Total aluminum	19.00 mgm/cm ² or 12.5 air cm.	11.8 air cm
Correction for Al	0.1 air cm	0.1 air cm
Air distance, collimator to detector	3.5 air cm	
Equivalent range, paraffin layer to detector air press. in atmos.)	32.7 cm × 741/760 (distance × mean	31.9 air cm
Equivalent range in 1st chamber: 8.7 cm × 1.6 × 1.1 (distance × O ₂ press. × O ₂ st. power)	15.3 air cm	15.3 air cm
Equiv. range to register in 2nd chamber:	0.2 air cm	0.2 air cm
Total: Minimum range necessary to cause coincidence:	31.6 air cm	59.3 air cm
Corresponding proton energy:	4.80 Mev	6.88 Mev

TABLE II. Calculation of neutron energies. $E_0 = E_{p0}/\cos^2\theta_0$, $E_4 = (E_{p1} + \Delta E_p)/\cos^2\theta_2$.

Run numbers	Cyclotron target	Al thickness, target (mils)	Al thickness, chamber (mils)	Proton energy (Mev)			Neutron energy (Mev)		
				Min. E_{p0}	Max. E_{p1}	Loss in paraffin ΔE_p	Min. E_0 ($\theta_0 = 23^\circ$)	Max. E_4 ($\theta_2 = 28.5^\circ$)	Effective value E
7, 10, 13	Be	0, 6	0-3	4.80	5.91	0.40	5.68	8.16	6.5
8, 9	Be	0	3-6	5.91	6.96	0.34	6.99	9.44	7.8
11, 12, 14, 15	Be	0	6-12	6.96	8.73	0.29	8.24	11.70	9.3
							($\theta_0 = 28.7^\circ$)	($\theta_2 = 34.1^\circ$)	
1, 16	Li	13	0-6	6.88	8.62	0.90	8.94	13.9	10.6
17	Li	13	6-12	8.62	10.16	0.78	11.2	15.9	12.8
2, 26	Li	12.5	6-13	8.62	10.40	0.78	11.2	16.3	12.9
3, 18	Li	11	12-19	10.16	11.74	0.70	13.2	18.1	14.8
4, 19	Li	8.5	18-25	11.53	12.86	0.63	15.0	19.6	16.5
5	Li	6	24-30	12.68	13.8	0.56	16.5	20.9	18.0
20, 23	Li	6	24-31	12.68	14.0	0.56	16.5	21.2	18.1
6, 25, 21	Li	3	30-38	13.8	15.2	0.50	17.9	22.9	19.6
22, 24	Li	0	36-46	14.9	16.4	0.45	19.4	24.6	21.1

pression for ΔT then becomes

$$\Delta T = [(C+D)/(C-D)^2 + (A+B)/(A-B)^2]^{1/2}$$

4. CORRECTIONS AND FINAL RESULTS

The procedure outlined above either eliminates or takes account of all significant random or accidental errors involved in the determination of the transmission fraction. Evidence for this is the fact that the differences in values of a cross section at a particular energy, obtained from runs on different days, and with different scatterer thicknesses, are in general not greater than the assigned standard deviations of these values (see Table III).

The method is subject to other errors the presence of which cannot be discovered by repeating measurements if, as was the case, the same geometry is used on all the occasions. The following four kinds of systematic errors may occur.

(a) Neutrons which leave the source in such a direction as not to hit the scatterers may be scattered into the detector by nearby objects such as the cyclotron magnet or the water wall. Though the water wall could be expected to absorb most of these neutrons, a test of the magnitude of this effect was made by putting 75 cm of paraffin between the neutron source and the detector. (Judging by the measurements on paraffin scatterers this reduced the number of neutrons in the beam by a factor of more than 300.) Counts were then taken at several different energy intervals, and at none of them was there

a significant difference between the number of coincidences observed with the lower limit absorber in place and that with the upper.

(b) Since the scatterer and the detector are not of negligible size compared to their distances from the source and from each other, some neutrons scattered by the scatterer will reach the detector. The magnitude of this effect was calculated as described below, and found to be such that the observed values of T are the order of 1 percent too large.

(c) The scatterer will also scatter into the detector a fraction of those neutrons which have already been scattered once by some object nearer the source. However, the intensity at the scatterer of such neutrons was much less than that of the direct beam from the source, because on only one side of the source-scatterer line was there anything sufficiently close and massive to scatter neutrons appreciably (a vertical section of the magnet yoke). Since this iron certainly had no focusing effect, the "apparent source" in it was much weaker than the actual source. Since the direct neutrons which the scatterer scattered into the detector made only about a 1 percent change in T , the effect of this sub-

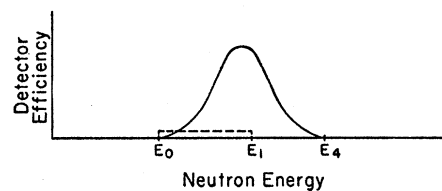


FIG. 2. Schematic diagram of detector efficiency as a function of neutron energy.

TABLE III. Calculation of total cross sections for carbon.

$\bar{\sigma}(C)$ = final value of total neutron-carbon cross section (elastic and inelastic scattering).
 $\Delta\sigma(C)$ = standard deviation in $\bar{\sigma}(C)$.
 T = transmission fraction corrected for scattering into detector.

Run number	Mean neutron energy (Mev)	Scatterer thickness (gd) (g/cm ²)	T_{obs}	T	ΔT (percent)	$\sigma(C)$ (10^{-24} cm ²)	$\Delta\sigma(C)$ (percent)	$\bar{\sigma}(C)$ (10^{-24} cm ²)	$\overline{\Delta\sigma}(C)$ (percent)
7	6.5	6.562	0.634	0.630	9.7	1.40	21		
10	6.5	10.936	0.432	0.428	9.6	1.54	11	1.51	10
8	7.8	6.562	0.596	0.592	10.4	1.59	19		
9	7.8	10.936	0.455	0.450	18	1.45	22	1.51	14
11	9.3	6.562	0.639	0.635	9.2	1.38	21		
12	9.3	10.936	0.450	0.446	10.1	1.47	12	1.45	10
1	10.6	13.123	0.395	0.390	9.5			1.43	10
2	12.9	10.936	0.499	0.494	10.9	1.28	15		
26	12.9	13.123	0.484	0.478	9.3	1.12	13	1.18	10
3	14.8	10.936	0.512	0.507	8.6			1.24	13
4	16.5	10.936	0.497	0.492	9.9			1.29	14
5	18.0	8.749	0.614	0.609	9.9			1.13	20
6	19.6	8.749	0.561	0.556	8.3	1.34	14		
25	19.6	15.311	0.376	0.370	9.8	1.30	10	1.31	8
24	21.1	13.123	0.468	0.462	7.4			1.17	10

stantially smaller number of indirect neutrons may be safely ignored.

(d) In those cases in which the upper limit of the energy interval was several Mev below the energy of the fastest neutrons produced by the source, the question arose whether some high energy neutrons might be scattered inelastically into the detector with an energy loss which would bring them into the working energy interval. Three major factors control the magnitude of this effect. In the first place, the total number of neutrons above the working interval was always smaller than the number in the interval, and most of these were within a few Mev of the upper limit of the interval. Secondly, Weisskopf¹¹ has shown that the mean energy after impact of neutrons in the 10–20-Mev range which suffer inelastic collisions is the order of one-third of their initial energy, so that only a small fraction lose less than 3 Mev. And finally, even if the angular distribution of the inelastically scattered neutrons had a pronounced maximum in the forward direction, the calculations described below show that only a small fraction of them would actually hit the detector. Thus it is clear that the contribution of inelastically scattered neutrons to the observed transmission fractions may be ignored.

To calculate the effect on the transmission

fractions of the neutrons scattered into the detector by the scatterer, it is necessary to know something about the angular distribution of the scattered neutrons, at least at small angles. For carbon (and larger) nuclei enough is known about this to make a calculation worth while. Placzek and Bethe¹² have suggested that the elastic scattering of fast neutrons by compound nuclei may be regarded as essentially a diffraction of the neutron beam by the nuclei, which correspond to absorbing disks or spheres in a beam of light. On this assumption the angular distribution of the elastically scattered neutrons is given by

$$K(\theta) = R^2 [J_1(kR\theta)/\theta]^2,$$

where $K(\theta)$ is the scattering cross section per unit solid angle at the angle θ , J_1 is a Bessel function of the first kind, k is the wave number of the incident neutrons, and R is the nuclear radius. The experimental results of Kikuchi, Aoki, and Wakatuki,¹³ who observed the angular distribution of 15-Mev neutrons scattered by various elements, agree very well with this expression (except for their measurements at 14° , the smallest angle at which they could work, which are probably in error).

¹² G. Placzek and H. A. Bethe, Phys. Rev. **57**, 1075A (1940).

¹³ S. Kikuchi, H. Aoki, and T. Wakatuki, Proc. Phys. Math. Soc. Japan **21**, 410 (1939); **22**, 430 (1940).

¹¹ V. F. Weisskopf, Phys. Rev. **52**, 295 (1937).

TABLE IV. Calculation of total cross sections for protons.

$\bar{\sigma}(H)$ = final value of total neutron-proton scattering cross section.
 $\sqrt{\sigma(H)}$ = standard deviation in $\bar{\sigma}(H)$.
 T = transmission fraction corrected for scattering into detector.

Run number	Mean neutron energy (Mev)	Scatterer thickness (x_d) (g/cm ²)	T_{obs}	T	ΔT (percent)	$\sigma(C)$ from Fig. 3 (10^{-24} cm ²)	$\sigma(H)$ (10^{-24} cm ²)	$\Delta\sigma(H)$ (percent)	$\bar{\sigma}(H)$ (10^{-24} cm ²)	$\overline{\Delta\sigma}(H)$ (percent)
13	6.5	6.302	0.302	0.300	6.3	1.56			1.40	8
14	9.3	6.302	0.414	0.410	5.2	1.44	0.90	10		
15	9.3	3.139	0.628	0.625	4.7	1.44	0.99	18	0.92	9
16	10.6	6.302	0.447	0.443	4.8	1.39			0.78	11
17	12.8	6.302	0.444	0.440	4.9	1.34			0.83	11
18	14.8	6.302	0.507	0.502	5.2	1.29			0.61	15
19	16.5	6.302	0.494	0.489	5.2	1.28			0.66	15
20	18.1	6.302	0.516	0.511	5.0	1.26	0.59	16		
23	18.1	3.163	0.746	0.743	4.5	1.26	0.45	33	0.55	14
21	19.6	6.302	0.539	0.533	5.3	1.25			0.52	18
22	21.1	6.302	0.576	0.569	5.0	1.25			0.41	21

The value of R to be used in the expression is related to the cross section σ_e for this elastic scattering by $\sigma_e = \pi R^2$. Since inelastic collisions also occur, σ_e is less than the total collision cross section, σ , calculable from the observed transmission fractions of the carbon scatterers. Sherr³ has compared the results of his experiments at 24 Mev, in which he also measured total cross sections, with those of Grahame and Seaborg¹ whose method was such that they measured cross sections for inelastic scattering only. Sherr finds strikingly good agreement between the results of the two kinds of experiments if he assumes $\sigma_e = \sigma_i = \frac{1}{2}\sigma$. It is reasonable from the point of view of the optical analogy, also, that the cross section for the diffraction process should be equal to the actual area of the disk.

On the basis of these assumptions the transmitted intensity was calculated (neutrons scattered once and twice by the scatterer were taken into account). The resulting expression for the observed transmission fraction is

$$T_{\text{obs}} = e^{-N\sigma x} \left[1 + \frac{A_s(l+h)^2}{l^2 h^2} \left(N\sigma_e x \frac{\bar{K}(\theta)}{\sigma_e} + \frac{(N\sigma_e x)^2 \bar{L}(\theta)}{2\sigma_e^2} + \dots \right) \right]$$

Here σ is the total and σ_e the elastic scattering cross section of carbon, Nx the number of atoms per cm² of scatterer, A_s the scatterer area (perpendicular to the beam), l and h the distances

from source to scatterer and from scatterer to detector, $\bar{K}(\theta)$ the average value of $K(\theta)$ as θ goes from 0° to 6° (6° is the largest value θ can have for particles which reach the detector, and $K(\theta)$ is nearly constant in this region), and $\bar{L}(\theta)$ the corresponding average value of the function $L(\theta)$ which gives the angular distribution of neutrons which have been scattered exactly twice.

For the three inch thick carbon scatterer and a neutron energy of 21 Mev, the second term in the bracket is 1.2 percent of the first term and the third is 0.17 percent of the first. Thus even at high energies, where the anisotropy of the scattering is greatest, this correction is small compared to the statistical fluctuations. However, since it changes all the cross sections in the same sense, it was computed roughly for each of the energies and scatterer thicknesses used, and applied to T_{obs} to get T as shown in Table III. The corrections to the paraffin transmission fractions indicated in Table IV were made in the same way with the additional assumption that scattering by the protons is isotropic in the center of gravity system. (Though this is very likely contrary to fact, there does not seem to be information now available which would make any other specific assumption more probable.)

The sixth column of Table III gives ΔT , the relative standard deviation in T , computed as described above from the observed numbers of counts. The column headed $\bar{\sigma}(C)$ gives the total collision cross section for carbon at each different

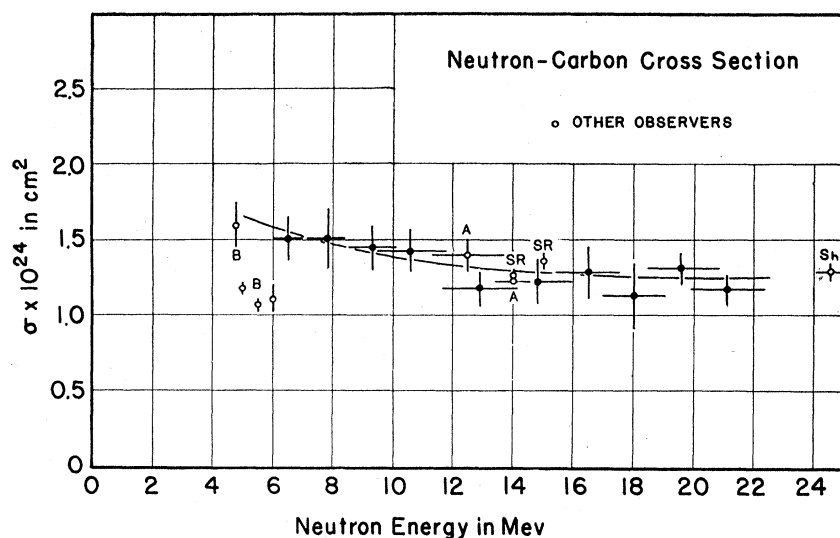


FIG. 3. Total neutron-carbon collision cross section as a function of energy. The length of the vertical line at each point is twice the standard deviation. The horizontal line indicates an energy range which contains about 0.8 of the neutrons in the interval. "B" represents Bailey *et al.*,⁵ "A" Ageno *et al.*,⁴ "SR" Salant and Ramsey,² and "Sh" Sherr.³

energy. The only significant contribution to $\overline{\Delta\sigma(C)}$, the relative standard deviation of $\bar{\sigma}(C)$, came from ΔT , since the standard deviation in Nx was less than 0.5 percent. In those cases in which two runs were made with the same energy interval, the columns headed $\sigma(C)$ and $\Delta\sigma(C)$ give the values for each run. $\bar{\sigma}(C)$ is the average of the two $\sigma(C)$ s, weighted according to their reliability.

The final values of the neutron-carbon collision cross sections, represented by solid dots, are plotted against energy in Fig. 3. The open circles show the results of other observers. (All available data above 5 Mev are plotted.) The total length of the vertical line is twice the standard deviation (resulting from statistical fluctuations) as computed above, in the case of the present experiments. For the other observers it is twice the stated uncertainty. The length of the horizontal line represents half of the total energy interval (in those cases where the information was available), and it is centered approximately at the effective value of the neutron energy. This part of the interval contained at least 0.8 of the total number of neutrons in the whole interval. Points marked "B" in Fig. 4 were obtained by Bailey *et al.*,⁵ those marked "A" by Ageno *et al.*,⁴ those marked "SR" by Salant and Ramsey,² and that marked "Sh" by Sherr.³

A value of $\sigma(C)$ for each energy interval must be used in the calculation of the proton cross section $\sigma(H)$ from measurements with paraffin

scatterers, and the question arises whether the best value at any energy is the actual result of the measurement at that energy, or the value lying on a smooth curve determined by all the points. The results of Bailey *et al.*⁵ suggest that the spacing of the virtual levels of the compound nucleus (about 0.3 Mev between maximum and minimum) is such that they would not be separated by the present experiments because of the large energy intervals which were used. Moreover, as the energy increases, one would expect the width of these levels to become greater compared to their separation in energy. Thus it is probable that the apparent fluctuations in $\sigma(C)$ are mainly due to the uncertainties in the measurement of the transmission fractions, and the value of $\sigma(C)$ used in the calculations of $\sigma(H)$ below were obtained from the smooth curve shown in Fig. 3.

For the paraffin scatterers the relation connecting the cross section with the corrected transmission fractions is

$$[\sigma(C) + f\sigma(H)]N_{Cx} = \log(1/T),$$

where f is the ratio of H atoms to C atoms (as evaluated in the previous section) and N_{Cx} is the number of C atoms per unit area of scatterer. The values of $\sigma(C)$ used at each energy are given in Table IV as well as the final values of the proton cross sections $\bar{\sigma}(H)$. In estimating the standard deviation in $\bar{\sigma}(H)$, the contributions of f and N_{Cx} have been ignored, and the standard

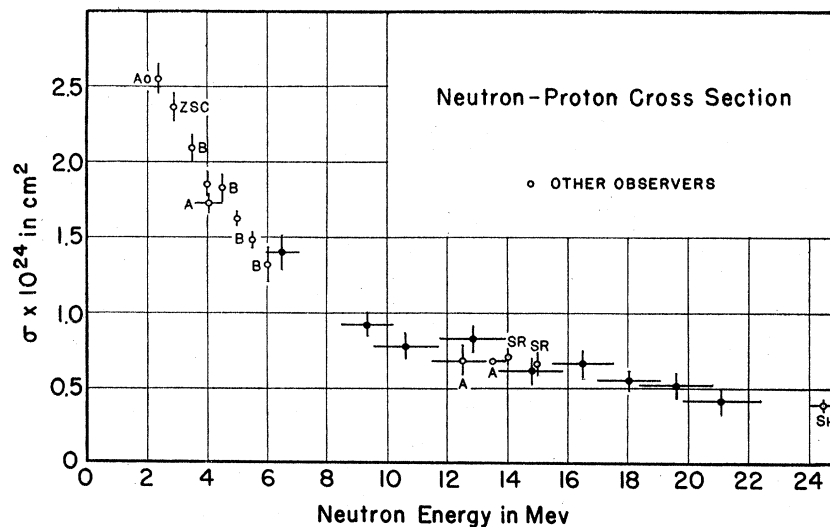


FIG. 4. Total neutron-proton collision cross section as a function of energy. Meaning of symbols as in Fig. 3. "A σ " represents Aoki¹⁴ and "ZSC" Zinn, Seely, and Cohen.¹⁵

deviation in the values of $\sigma(C)$ read from the curve was assumed to be about 5 percent. In Fig. 4 the final values of $\bar{\sigma}(H)$ and also the results of other observers (complete above 3 Mev) are plotted against energy. The symbols here, including the initials representing other observers, have the same meanings as in Fig. 4. "A σ " and "ZSC" (which did not appear before) indicate, respectively, Aoki¹⁴ and Zinn, Seely, and Cohen,¹⁵ who both used D-D neutrons of sharply defined energy.

5. DISCUSSION

Because of the uncertain state of theories of nuclear radii, a comparison with them of measured cross sections of a single nucleus is of little significance. For this purpose measurements at a single energy on several nuclei differing widely in mass, such as those carried out by Sherr,³ are much more useful. Thus the actual values of the carbon cross sections resulting from the present experiments are of interest principally because of the comparisons they allow, at those energies which have been previously used, with the experimental results obtained by other observers using different methods. As can be seen from Fig. 3, in which all the available data above 5 Mev have been plotted, the results of the present experiments agree with those of other observers above 6 Mev within experimental error.

¹⁴ H. Aoki, Phys. Rev. 55, 795 (1939).

¹⁵ W. H. Zinn, S. Seely, and V. W. Cohen, Phys. Rev. 56, 260 (1939).

In the previous section a theory was mentioned according to which the elastic scattering of fast neutrons by compound nuclei may be regarded as essentially a diffraction of the neutron beam by the nuclei. This picture should begin to be valid at energies such that the wavelength of the neutron beam is small compared to nuclear dimensions. At 15 Mev, for example, $\lambda = 1.2 \times 10^{-13}$ cm, and $R = 4.5 \times 10^{-13}$ cm. R is the "geometrical radius" of a carbon nucleus computed on the assumption discussed above, that the cross sections for elastic and inelastic scattering are equal so that $\sigma(C) = 2\pi R^2$. Under these conditions, resonances will have a relatively small effect on the total cross section and one would expect the latter to be essentially independent of energy. This expectation is borne out by the experimental results shown in Fig. 3, which indicate that the average cross section over 2-Mev intervals changes very little between 15 and 25 Mev.

The experimental results for the total neutron-proton cross section, and also the predictions of several theories, are summarized in Table V in such a way as to facilitate comparisons.

Column 1 of Table V indicates the energies at which the cross sections have been evaluated. Column 2 contains values of σ_{exp} read from a smooth monotonically decreasing curve through the center of the region covered by the experimental points shown in Fig. 4. All the available data above 2 Mev have been considered. None

TABLE V. Comparison of measured proton cross sections with the results of various theories.

(1)	(2)	(3)	(4)	(5)	(6)	(7)	(8)
E (Mev)	σ_{exp} (10^{-24} cm^2)	σ_W	σ_{Wa}	σ_{KB} (s wave)	σ_{RSI}	σ_{RSII}	σ_{RSIII}
Theoretical cross sections (10^{-24} cm^2)							
2.5	2.60	2.18	2.57	2.74	2.69	2.69	2.69
4.0	1.91	1.56	1.94	2.02	2.05	2.05	2.05
6.0	1.39	1.18	1.49	1.48	1.52	1.52	1.55
8.0	1.08	0.95	1.22	1.16	1.19	1.20	1.32
10.0	0.90	0.80	1.03	0.94	0.96	0.98	1.18
12.0	0.78	0.69	0.89	0.77	0.80	0.83	1.08
14.0	0.69	0.61	0.79	0.66	0.68	0.72	1.01
16.0	0.61	0.55	0.71	0.57	0.59	0.64	0.97
18.0	0.55	0.49	0.64	0.50	0.53	0.58	0.94
20.0	0.50	0.45	0.59	0.44	0.48	0.53	0.92
22.0	0.45	0.41	0.54	0.40	0.44	0.48	0.91
24.0	0.41	0.38	0.50	0.37	0.41	0.45	0.91

of the experimental points lies off the curve by more than 11 percent of its ordinate. In general, it would be safer to compare each of the theoretical curves directly with the data. However, since all the theoretical curves have the same character as the one drawn through the data, and since it is not necessary to distinguish between two theoretical curves which fit well over the whole range, the present method of comparison is probably adequate.

In column 3 of Table V are given values of the cross section computed from the Wigner formula

$$\sigma_W = \frac{\pi \hbar^2}{M} \left[\frac{3}{\frac{1}{2}E + |\epsilon|} + \frac{1}{\frac{1}{2}E + |\epsilon'|} \right]. \quad (1)$$

The energies taken for the triplet and singlet levels of the neutron-proton system are $\epsilon = 2.18$ Mev, $\epsilon' = 0.072$ Mev. The value of ϵ' was computed by substituting into Eq. (1) the experimental value of σ for very slow neutrons (1–10 ev) obtained by Hanstein,¹⁶ i.e., $\sigma_0 = 20 \times 10^{-24}$ cm^2 . The values of σ predicted by Eq. (1) are too small throughout the energy range. However, beyond 4 Mev they come closer to the experimental values with increasing energy, and at the high energy end agree within 7 percent. There may be some significance in the fact that above 18 Mev this expression, based on the simple assumption that the range of the forces is zero, fits the data better than any of the other theories except the "symmetrical" one of Rarita and Schwinger (column 6). Column 4 of Table V

¹⁶ H. B. Hanstein, Phys. Rev. 57, 1045 (1940).

contains values of σ obtained from the Wigner formula, modified by the inclusion of the first power of the range a of the forces. The value which was assumed here is $a = 2.0 \times 10^{-13}$ cm.

$$\sigma_{Wa} = \frac{\pi \hbar^2}{M} \left[\frac{3(1 + a(M|\epsilon|)^{1/2}/\hbar)}{\frac{1}{2}E + |\epsilon|} + \frac{1 - a(M|\epsilon'|)^{1/2}/\hbar}{\frac{1}{2}E + |\epsilon'|} \right]. \quad (2)$$

This expression, and the experimental value of σ for very slow neutrons given in the previous paragraph, lead to a value of 0.069 Mev for ϵ' . The resulting values of σ_{Wa} agree well with experiment up to about 6 Mev, but at higher energies the agreement is not so good as that of the simple Eq. (1). If in the above formula, a is set equal to 2.8×10^{-13} cm, the range of force suggested by proton-proton scattering, the resulting values of σ are about 10 percent larger than those in column 4, and differ from the data correspondingly more.

The results of Kittel and Breit¹⁷ are given in column 5 of Table V. These authors assumed a square potential well of radius $a = 2.8 \times 10^{-13}$ cm, and, retaining the first four powers of this radius, obtained expressions for the total S -wave scattering cross section. These values are in fairly good agreement with the experimental results in the low and middle energy range, but above 14 Mev are too small. On the assumption that the S -wave potential well is independent of energy, this difference gives an indication of the magnitude of the P -wave scattering cross section, i.e., about 0.03×10^{-24} cm^2 at 16 Mev, and 0.04×10^{-24} cm^2 at 24 Mev.

Kittel and Breit have calculated the P -wave cross section on the basis of Bethe's neutral form of meson theory and obtain $\sigma_{P \text{ wave}} = 0.12 \times 10^{-24}$ cm^2 for a meson mass $\mu = 177m$, and 0.01×10^{-24} cm^2 for $\mu = 330m$, as suggested by proton-proton scattering. The magnitude of the P -scattering has also been calculated by Smorodinsky¹⁸ from the angular distribution data of Amaldi and associates⁸ by a direct method involving no meson theory and no assumption about the shape of the interaction potential. For a neutron

¹⁷ C. Kittel and G. Breit, Phys. Rev. 56, 744 (1939).

¹⁸ J. Smorodinsky, J. Phys. U.S.S.R. 8, 219 (1944).

energy of 16 Mev he obtains $\sigma_{P \text{ wave}} = 0.01 \times 10^{-24}$ cm², in fair agreement with the observed value assuming Kittel and Breit's *S*-wave cross section.

The last three columns of Table V contain estimates accurate to about 1 percent of the total cross sections predicted by the three theories of Rarita and Schwinger¹⁹ (I "symmetrical," II "charged," and III "neutral"). The tabulated values in each column were read from a smooth curve drawn through five computed values (at 2.8, 6, 10, 15.3, and 25 Mev) of the cross section predicted by the corresponding theory.²⁰ The experimental values agree fairly well with the results of the "symmetrical" theory throughout the energy range, and very well

above 12 Mev. Of the theories considered, this one gives the best over-all fit. The "neutral" theory, on the other hand, fits so poorly as to be unequivocally eliminated by the data. The "charged" theory differs consistently and significantly from the experimental results, and is at best an unlikely possibility.

The author wishes to express his gratitude to Professors H. R. Crane and G. E. Uhlenbeck for their interest and advice throughout the course of this work, and to Professor J. M. Cork, whose direction of the Michigan Cyclotron Laboratory made these experiments possible. He is also indebted to Mr. Wayne Middleton and to the other members of the cyclotron crew for their unflinching cooperation. The cyclotron operating expenses were met by a grant from the Horace H. Rackham Fund.

¹⁹ W. Rarita and J. Schwinger, *Phys. Rev.* **59**, 556 (1941).

²⁰ The author is indebted to Dr. C. L. Critchfield for suggestions concerning these calculations.

The Vector Mesotron

JAMES H. BARTLETT

Department of Physics, University of Illinois, Urbana, Illinois

(Received April 15, 1947)

The wave equations of Proca for a vector mesotron (spin 1) are specialized first to the case in which there is no magnetic field, and then to that in which the field is central. The wave functions satisfy fourth-order homogeneous differential equations. For the states $l=j\pm 1$, it is simpler to consider two simultaneous second-order differential equations in two unknowns (see Eqs. (19) and (21) of this article). For a coulomb field, the form of the radial functions at $r=0$ is established as $u = \exp[-aL/r^{\frac{1}{2}}]r^{\beta}f$, where $a=2(z\alpha)^{\frac{1}{2}}[j(j+1)]^{\frac{1}{2}}$, $L^2 = \hbar/Mc$, M =rest mass of mesotron, f is an ascending power series in r , ze is the charge on the coulomb source, α is the fine-structure constant $e^2/\hbar c$, and β is a constant which can be determined.

INTRODUCTION

CORBEN and Schwinger¹ and, independently, Tamm^{2,3} have discussed the stationary states of a vector mesotron in a coulomb field. Corben and Schwinger have written down the explicit radial equations when $l=j\pm 1$, and Tamm² has indicated the general nature of the solution. It is the purpose of the present article to give further details of the solution, together with its derivation. The notation of Corben and Schwinger will be adopted.

WAVE EQUATION

The wave equations of Proca⁴ for a vector mesotron in an external field with a four-potential A_α

¹ H. C. Corben and J. Schwinger, *Phys. Rev.* **58**, 953 (1940).

² I. Tamm, *Phys. Rev.* **58**, 952 (1940).

³ I. Tamm, *Comptes Rendus U.S.S.R.* **29**, 551 (1940).

⁴ See N. Kemmer, *Proc. Roy. Soc.* **A166**, 133 (1938).